ChemComm

Accepted Manuscript

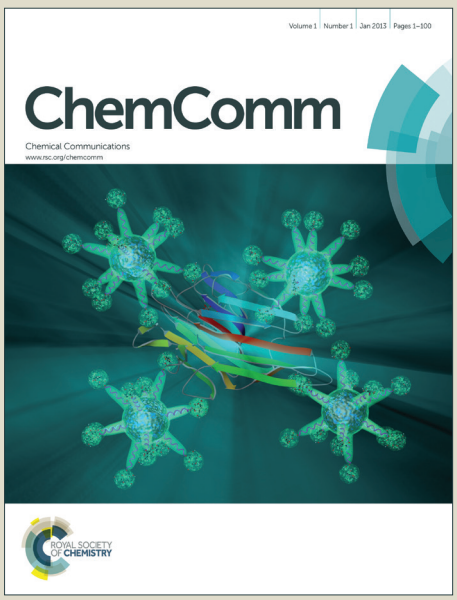

ROYAL SOCIETY OF CHEMISTRY

www.rsc.org/chemcomm

Cite this: DOI: 10.1039/c0xx00000x

www.rsc.org/xxxxxx

ARTICLE TYPE

Facile fabrication of microsphere-polymer brush hierarchically three-dimensional (3D) substrates for immunoassays

Jiao Ma, [a,b] Shifang Luan,*[a] Lingjie Song,[a] Shuaishuai Yuan, [a,b] Shunjie Yan, [a,b] Jing Jin [a] and Jinghua Yin*[a]

Received (in XXX, XXX) Xth XXXXXXXXX 20XX, Accepted Xth XXXXXXXXX 20XX
DOI: 10.1039/b000000x

Abstract: We propose a facile UV strategy to construct a hierarchically three-dimensional (3D) substrate that comprises a polystyrene (PS) microsphere layer on cycloolefin polymer (COP) substrate and densely packed hydrophilic polymer brushes grafting from this 3D backbone. This hierarchical substrate enables the high antibody loading capacity, 3D manner of analyte capture, therefore enhancing detection signal while reducing background noise.

Highly sensitive immunoassays have shown great potential in the field of biomedical diagnosis, food inspection and environmental monitoring.[1] Surface properties including surface structure and surface chemistry are especially primary factors that control the sensitivity of immunoassays.[2] To improve the performance of immunoassays, various substrates have been specifically designed.[3] Due to the huge surface area and the high probe loading capacity, many nanomaterials such as carbon nanotubes, zinc oxide nanorods, and even virus nanoparticles have been employed to construct three-dimensional (3D) nanostructured substrates for enhancing detection signal.[4] However, extra procedures are usually required to covalently or electrostatically immobilize the nanoparticles onto the substrates. Moreover, the high probe loading capacity originating from the large surface area is accompanied by the intensive nonspecific protein adsorption which will result in the increased background noise. Thus, it is challenging to create a functionalized 3D substrate which can enhance the loading of capture probes while suppressing nonspecific protein adsorption.

Polymer brushes have been reported as an antifouling layer on a hydrophobic two-dimensional (2D) substrate, meanwhile obviously increasing the loading capacity of antibodies.[1b, 2a, 5] A hierarchically 3D substrate that was fabricated through combining 3D substrates and densely packed polymer brushes, will present a highly sensitive detection signal while low background noise; however, the related work is still very rare.[6] Until recently, Hu et al. reported a hierarchically nanostructured organic-inorganic hybrid substrate that enabled highly sensitive detection of cancer biomarker in human serum.[6] The complex procedure started with the growth of ZnO nanorods on slides, followed by attachment of initiator molecules, 2-bromoisobutyryl bromide, with (3-aminopropyl) triethoxysilane as a linker, and then growth of poly(oligo(ethylene glycol) methacrylate-*co*-glycidyl methacrylate) brushes via surface-initiated atom transfer radical polymerization under oxygen-free conditions.

Herein, for the first time, we report a facile and robust UV strategy to construct a hierarchically 3D substrate that consists of a polystyrene (PS) microsphere layer on a cycloolefin polymer (COP) substrate and densely packed hydrophilic polymer brushes grafting from the 3D backbone for immunoassays (scheme 1). The PS microspheres layer serves as a 3D backbone, to grow the high-density polymer brushes and facilitate more frequent antibody-antigen binding on the 3D solid/liquid interfaces. While the hydrophilic polymer brush, poly(2-hydroxyethyl methacrylate-*co*-2-carboxyethyl acrylate) (p(HEMA-*co*-CEA)), can resist the nonspecific protein adsorption, immobilize high-density antibodies, and preserve the native bioactivities of antibodies.

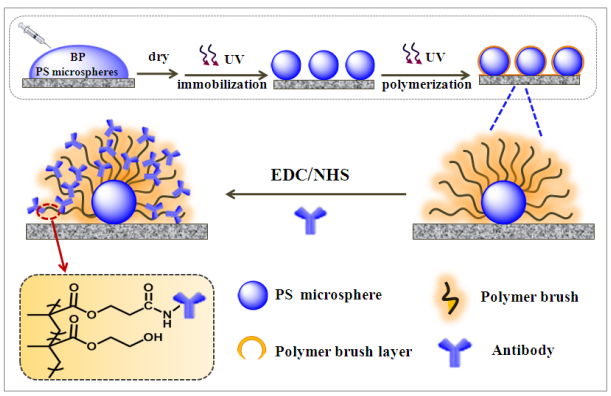

Scheme 1. Preparation of microsphere-polymer brush hierarchically 3D substrates via a two-step UV irradiation procedure.

As shown in scheme 1, the microsphere-polymer brush hierarchically 3D substrate was simply fabricated through two-step UV irradiation at ambient temperature for several minutes without expensive reagents and strict operations to remove water and oxygen. The first UV irradiation was used to immobilize the PS microspheres (for detail, see ESI†). When excited by UV light, benzophenone (BP) photoinitiators abstracted the hydrogens of C-H bonds of the COP substrate and PS microspheres,[7] and the resultant carbon-centered radicals were coupled together, therefore leading to the covalent immobilization of the PS microspheres onto the COP substrate. The as-prepared 3D surface

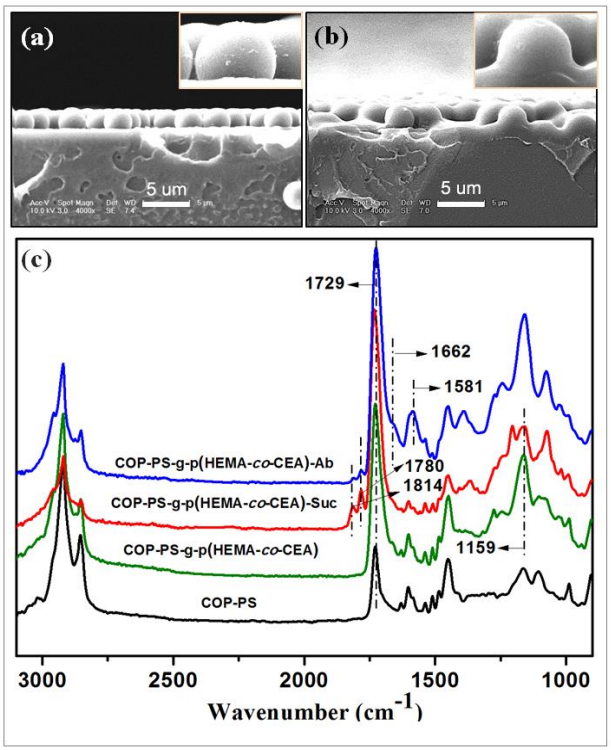

Fig. 1 SEM images of the cross sectional view for COP-PS supports (a) before and (b) after photografting polymerization, (c) ATR-FTIR spectra of the samples.

was stable throughout the immunoassay experiment. As scanning electron microscopy (SEM) images of the cross-sectional view (Fig. 1a) and the top-view (Fig. S1a and b) shown, a monolayer of PS microspheres in a non-closed packing pattern, randomly distributed on the COP surface, thus allowing more antibodies to be attached because of the greatly increased surface area. Then, the microsphere-polymer brush hierarchically 3D substrates were constructed through a facile UV surface-initiated graft polymerization. This graft polymerization strategy is particularly attractive mainly due to its short grafting time, high grafting density, easy operation and mild conditions.[8] Comparing with the COP-PS surface, two obvious adsorption peaks at 1729 cm^{-1} (C=O, stretching vibration) and 1159 cm^{-1} (C-OH, stretching vibration) attributing to the p(HEMA-*co*-CEA) polymer brushes in attenuated total reflectance-Fourier transform infrared spectroscopy (ATR-FTIR) curves were detected on the p(HEMA-*co*-CEA)-modified hierarchically 3D substrates (COP-PS-g-p(HEMA-*co*-CEA)) (Fig. 1c). In addition, we observed that a soft polymer layer fully covered the PS microspheres surfaces and the exposed COP substrates after the photografting polymerization, and the coatings on adjacent microspheres even merged together (Fig. 1b, Fig. S1c and d). The surface roughness of the samples was quantitatively examined by atom force microscopy (AFM) (Fig. S2). The root mean square (RMS) roughness for the virgin 2D COP substrate was only ~4.8 nm, and it increased slightly to ~11.8 nm when grafting polymer brushes. In contrast, the RMS for the PS microsphere-modified 3D COP substrate (COP-PS) was ~126.3 nm, and it dramatically reached up to ~265.7 nm with the introduction of polymer brushes. The amount of surface carboxyl groups was determined by a colorimetric method using Toluidine Blue (TB) solution.[9] We found that it correspondingly increased as the photografting time increased from 3 min to 12 min, and the hierarchically 3D substrates demonstrated much larger values than the polymer brush-modified 2D substrates (Fig. S3). The hierarchically 3D substrates had the prominent surface properties, e.g., the dramatically enhanced roughness and highly dense carboxyl moieties, therefore providing a suitable platform for attaching high-density antibodies and efficient access of antigens in immunoassays.

To evaluate the immunoassay performances, A555-labeled anti-rabbit IgG was first immobilized onto the hierarchically 3D substrate through a simple 1-ethyl-3-(3-dimethylaminopropyl)-carbodiimide and N-hydroxysuccinimide (EDC/NHS) chemistry.[10] As shown in Fig. 1c, two peaks at 1814 and 1780 cm^{-1} belonging to the succinimidyl ester structure confirmed the activation of carboxyl groups. The amide I and amide II structures (at about 1662 and 1581 cm^{-1}**)** were observed with the introduction of antibodies. For comparison, the virgin COP substrate, the COP-PS substrate, and the p(HEMA-*co*-CEA)-modified COP substrate (COP-g-p(HEMA-*co*-CEA)) were used as references (Fig. 2A). It should be noted that as for COP and COP-PS references, antibodies were physically adsorbed on the substrates, which was different from the chemical immobilization of antibodies on COP-PS-g-p(HEMA-*co*-CEA) and COP-g-p(HEMA-*co*-CEA) via the EDC/NHS chemistry. These samples were examined by a confocal laser scanning microscope (CLSM), and the fluorescence images and mean fluorescence intensities were collected (Fig. S4 and Fig. 2B). As for the mean fluorescence intensity, the highest value of ~748 a.u, was detected on COP-PS-g-p(HEMA-*co*-CEA) substrate, which was as 31-fold, 6.6-fold and 3.5-fold high as on COP, COP-g-p(HEMA-*co*-CEA), and COP-PS, respectively. The flexible polymer brushes with high-density carboxyl groups that can bind antibodies and the PS microsphere 3D backbone with a large surface area synergistically contributed to the dramatically enhanced antibody loading on the COP-PS-g-p(HEMA-*co*-CEA) substrate, relative to the virgin COP substrate. The antibody-immobilized substrates were then subjected to antigen recognition. The highest detection signal was observed on COP-PS-g-p(HEMA-*co*-CEA) substrate (Fig. S4 and S5). Furthermore, the p(HEMA-*co*-CEA) polymer brush microarrays were respectively fabricated on the virgin COP and COP-PS substrates for visually investigating the effect of PS microsphere 3D backbone on antigen recognition. After the antibody-immobilized COP-g-p(HEMA-*co*-CEA) and COP-PS-g-p(HEMA-*co*-CEA) microarrays specifically interacted with target antigen, the uniform and strong green fluorescence microarray images on the COP-PS-g-p(HEMA-*co*-CEA) sample were observed, in contrast to the dark and vague fluorescence images on the COP-g-p(HEMA-*co*-CEA) surface (Fig. 2C). These results confirmed that not only did the immobilized antibody specifically recognize its target antigen, but also the COP-PS-g-p(HEMA-*co*-CEA) sample had a much higher capability of antigen recognition relative to the COP-g-p(HEMA-*co*-CEA) reference.

As mentioned above, the high probe loading capacity for the hydrophobic nanostructured substrate is accompanied by strong

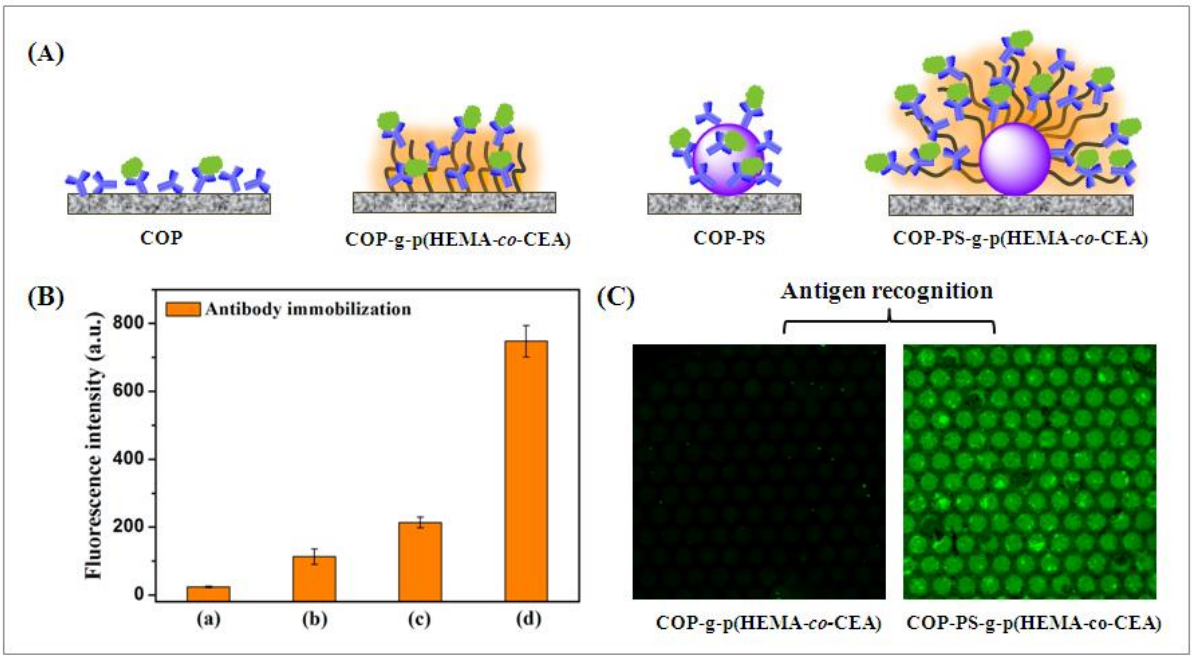

Fig. 2 (A) Schematic of different substrates used for comparison, (B) mean fluorescence intensity for antibody immobilization on the substrates: (a) COP, (b) COP-g-p(HEMA-*co*-CEA), (c) COP-PS, (d) COP-PS-g-p(HEMA-*co*-CEA), (C) fluorescence microarray images for antigen recognition on the supports.

nonspecific protein adsorption. The as-prepared microsphere-polymer brush 3D hierarchical substrate is expected to solve this contradiction. Herein, the nonspecific protein adsorption was investigated by directly exposing the substrates to the 100 μg/mL A488-labeled fibrinogen solution. The relative amount of protein adsorption respectively decreased by 40% and 90% on the COP-PS-g-pCEA and COP-PS-g-pHEMA samples, relative to the COP-PS samples, presenting the good antifouling performances for the polymer brushes, especially for the pHEMA brushes that possess lots of -OH groups (Fig. S6). The p(HEMA-*co*-CEA) polymer brushes grafting from the COP-PS substrate enable both excellent antifouling performance and a high loading capacity. Furthermore, for investigating the effect of polymer brushes, both of the antibody-immobilized COP-PS-g-p(HEMA-*co*-CEA) and COP-PS supports were respectively incubated in the A488-fibrinogen solution (100 μg/mL) and A488-avidin antigen solution (1 μg/mL), and the samples were examined by CLSM under the same conditions. Weak fluorescence for nonspecific protein adsorption at a high concentration of 100 μg/mL, while strong fluorescence for specific antigen recognition even at a much lower concentration of 1 μg/mL were observed on the COP-PS-g-p(HEMA-*co*-CEA) supports, which is in contrast to the COP-PS supports (Fig. 3a). In detail, the amount of nonspecific protein adsorption on the antibody-immobilized COP-PS-g-p(HEMA-*co*-CEA) supports decreased by ~70% compared with the COP-PS supports. Although the capability of antigen recognition has increased by dozens of times with the introduction of PS microsphere backbone (Fig. S5), the detection signal on the COP-PS-g-p(HEMA-*co*-CEA) supports further increased to more than three times that on the COP-PS supports (Fig. 3b). The performance of polymer brushes was comparable to the previously reported result, a two-fold increase in antigen recognition.[2a] To detect a specific disease marker in practice, due to the presence of high concentrations of nontarget proteins in sera (noise), the nonspecific adsorption of these nontarget molecules decrease the of analyte (signal) while increasing the background noise, thereby reducing assay confidence. The ratio of fluorescence intensity for specific antigen recognition to that for nonspecific protein adsorption ($R_{sp/nsp}$) was popularly used to

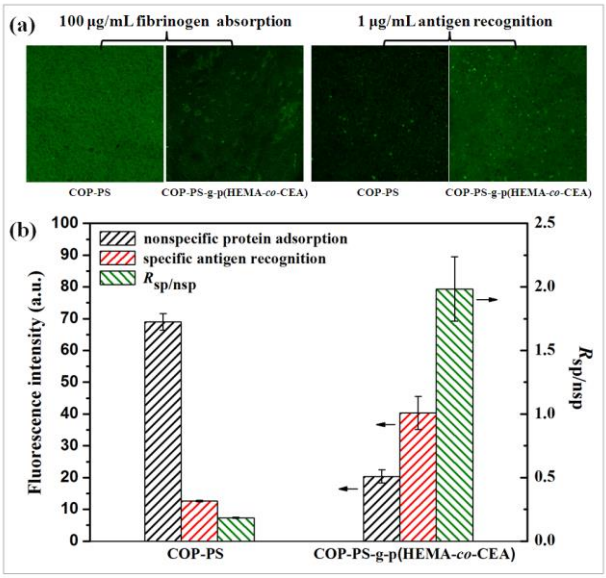

Fig. 3 (a) Fluorescence images for the antibody-immobilized supports after incubating in A488-fibrinogen or antigen solution, (b) fluorescence intensity for nonspecific protein adsorption and specific antigen recognition, and the $R_{sp/nsp}$ value on the supports.

evaluate the signal-to-noise (S/N) value.[5a] The $R_{sp/nsp}$ value for

hierarchically 3D COP-PS-g-p(HEMA-*co*-CEA) supports was as 10-fold high as that for COP-PS supports, because of both the high loading capacity of antibodies and good antifouling property of the p(HEMA-*co*-CEA) polymer brush.

In conclusion, a facile and robust strategy based on UV irradiation was developed to create a hierarchically 3D substrate consisting of a PS microsphere backbone layer and a densely packed hydrophilic p(HEMA-*co*-CEA) polymer brush layer for immunoassays, which synergistically contributed to the high antibody loading capacity and enhanced detection signal while reducing background noise. Moreover, the facile UV strategy can be easily conducted without time-consuming and harsh operations, expensive reagents and devices. Although the COP substrate and PS microsphere were used as a proof of concept in this study, this strategy should be applicable to a wide range of polymer substrates and nanoparticles containing C-H groups. This research demonstrated the hierarchically 3D substrate with tunable surface chemistry via a facile UV approach has a great potential application in various bioassays, especially in the early diagnosis of diseases.

The authors acknowledge financial support of the National Natural Science Foundation of China (Projects 21274150 and 51273200), Chinese Academy of Sciences-Wego Group High-tech Research & Development Program (ZKYWG2013-01).

[a] *State Key Laboratory of Polymer Physics and Chemistry, Changchun Institute of Applied Chemistry, Chinese Academy of Sciences, Changchun 130022, China. Email: sfluan@ciac.ac.cn, yinjh@ciac.ac.cn*

[b] *University of the Chinese Academy of Sciences, Beijing 100039, P.R. China.*

† Electronic Supplementary Information (ESI) available: Details of fabrication of hierarchically 3D substrates, top-view SEM images, AFM images, optical density of TB solutions versus grafting time, fluorescence images for antibody immobilization and antigen recognition, the fluorescence intensity for antigen recognition on the substrates and the antifouling performance of substrates. See DOI: 10.1039/b000000x/

Notes and references

1 (a) W. Hu, Y. Liu, Z. Lu and C. M. Li, *Adv. Funct. Mater*., 2010, **20**, 3497; (b) A. Hucknall, D. H. Kim, S. Rangarajan, R. T. Hill, W. M. Reichert and A. Chilkoti, *Adv. Mater*., 2009, **21**, 1968; (c) Y. M. Wu, Y. Cen, L. J. Huang, R. Q. Yu and X. Chu, *Chem. Commun*., 2014, **50**, 4759; (d) S. Song, Y. Qin, Y. He, Q. Huang, C. Fan and H. Y. Chen, *Chem. Soc. Rev*., 2010, **39**, 4234; (e) V. Gubala, L. F. Harris, A. J. Ricco, M. X. Tan and D. E. Williams, *Anal. Chem.*, 2012, **84**, 487.

2 (a) C. J. Huang, N. D. Brault, Y. Li, Q. Yu and S. Jiang, *Adv. Mater*., 2012, **24**, 1834; (b) K. Chuah, L. M. Lai, I. Y. Goon, S. G. Parker, R. Amal and J. J. Gooding, *Chem. Commun*., 2012, **48**, 3503; (c) J. Y. Eum, S. Y. Hwang, Y. Ju, J. M. Shim, Y. Piao, J. Lee, H.S. Kim and J. Kim, *Chem. Commun*., 2014, **50**, 3546; (d) V. Gubala, X. Le Guevel, R. Nooney, D. E. Williams and B. MacCraith, *Talanta*, 2010, **81**, 1833.

3 (a) R. P. Gandhiraman, C. Volcke, V. Gubala, C. Doyle, L. B. Desmonts, C. Dotzler, M. F. Toney, M. Iacono, R. I. Nooney, S. Daniels, B. James and D. E. Williams, *J. Mater. Chem.*, 2010, **20**, 4116; (b) N. Lu, A. R. Gao, P. F. Dai, S. P. Song, C. H. Fan, Y. L. Wang and T. Li, *Small*, 2014, **10**, 2022; (c) V. Gubala, N. C. H. Le, R. P. Gandhiraman, C. Coyle, S. Daniels and D. E. Williams, *Colloids Surf., B*, 2010, **81**, 544.

4 (a) R. Akter, M. A. Rahman and C. K. Rhee, *Anal. Chem.*, 2012, **84**, 6407; (b) J. S. Park, M. K. Cho, E. J. Lee, K. Y. Ahn, K. E. Lee, J. H. Jung, Y. Cho, S. S. Han, Y. K. Kim and J. Lee, *Nat. Nanotechnol.*, 2009, **4**, 259; (c) K. Y. Ahn, K. Kwon, J. Huh, G. T. Kim, E. B. Lee, D. Park and J. Lee, *Biosens. Bioelectron*., 2011, **28**, 378.

5 (a) L. Song, J. Zhao, S. Luan, J. Ma, J. Liu, X. Xu and J. Yin, *ACS Appl. Mater. Interfaces*, 2013, **5**, 13207; (b) J. Ma, S. Luan, L. Song, J. Jin, S. Yuan, S. Yan, H. Yang, H. Shi and J. Yin, *ACS Appl. Mater. Interfaces*, 2014, **6**, 1971; (c) N. Zhang, T. Pompe, I. Amin, R. Luxenhofer, C. Werner and R. Jordan, *Macromol. Biosci*., 2012, **12**, 926.

6 W. Hu, Y. Liu, T. Chen, Y. Liu and C. M. Li, *Adv. Mater*., 2015, **27**,181.

7 (a) J. Xu, Y. Ma, J. Xie, F. J. Xu and W. Yang, *J. Polym. Sci., Part A: Polym. Chem.*, 2011, **49**, 2755; (b) C. Li, F. Xu and W. Yang, *Langmuir*, 2013, **29**, 1541; (c) M. Toma, U. Jonas, A. Mateescu, W. Knoll and J. Dostalek, *J. Phys. Chem. B*, 2013, **117**, 11705.

8 (a) J. Chen, P. Xiao, J. C. Gu, D. Han, J. W. Zhang, A. H. Sun, W. Q. Wang and T. Chen, *Chem. Commun*., 2014, **50**, 1212; (b) U. Edlund, S. Danmark and A. C. Albertsson, *Biomacromolecules*, 2008, **9**, 901; (c) P. Xiao, J. Gu, J. Chen, D. Han, J. Zhang, H. Cao, R. Xing, Y. Han, W. Wang and T. Chen, *Chem. Commun*., 2013, **49**, 11167; (d) S. F. Luan, J. Zhao, H. W. Yang, H. C. Shi, J. Jin, X. M. Li, J. C. Liu, J. W. Wang, J. H. Yin and P. Stagnaro, *Colloids Surf., B*, 2012, **93**, 127; (e) U. Edlund, M. Källrot and A. C. Albertsson, *J. Am. Chem. Soc.*, 2005, **127**, 8865; (f) P. Xiao, J. C. Gu, J. Chen, J. W. Zhang, R. B. Xing, Y. C. Han, J. Fu, W. Q. Wang and T. Chen, *Chem. Commun*., 2014, **50**, 7103.

9 K. N. Chua, W. S. Lim, P. C. Zhang, H. F. Lu, J. Wen, S. Ramakrishna, K. W. Leong and H. Q. Mao, *Biomaterials*, 2005, **26**, 2537.

10 H. Vaisocherová, W. Yang, Z. Zhang, Z. Cao, G. Cheng, M. Piliarik, J. i. Homola and S. Jiang, *Anal. Chem.*, 2008, **80**, 7894.